

## Competitive reaction and quenching of vibrationally excited $O^+ 2$ ions with $SO_2$ , $CH_4$ , and $H_2O$

M. DurupFerguson, H. Böhringer, D. W. Fahey, F. C. Fehsenfeld, and E. E. Ferguson

Citation: *The Journal of Chemical Physics* **81**, 2657 (1984); doi: 10.1063/1.447975

View online: <http://dx.doi.org/10.1063/1.447975>

View Table of Contents: <http://scitation.aip.org/content/aip/journal/jcp/81/6?ver=pdfcov>

Published by the AIP Publishing

---

### Articles you may be interested in

Rate constants for the reactions of metastable  $NO^+$  ( $a 3\Sigma^+$ ) ions with  $SO_2$ ,  $CO_2$ ,  $CH_4$ ,  $N_2$ , Ar,  $H_2$ ,  $D_2$ , and  $O_2$  at relative kinetic energies 0.04–2.5 eV

*J. Chem. Phys.* **71**, 3280 (1979); 10.1063/1.438758

Quenching of vibrationally excited  $N_2$  by  $SO_2$

*J. Chem. Phys.* **68**, 2014 (1978); 10.1063/1.435890

Excitation and quenching reactions in Ebeam excited He/ $H_2O$  and He/ $CH_3CN$  systems

*J. Chem. Phys.* **68**, 538 (1978); 10.1063/1.435763

Erratum: Temperature dependence of the quenching of vibrationally excited  $N_2$  by NO and  $H_2O$

*J. Chem. Phys.* **67**, 2398 (1977); 10.1063/1.435443

Chemiluminescence of CH in the  $O + C_2H_2$  Reaction : Rotational Relaxation and Quenching

*J. Chem. Phys.* **46**, 7 (1967); 10.1063/1.1840432

---



# Competitive reaction and quenching of vibrationally excited $O_2^+$ ions with $SO_2$ , $CH_4$ , and $H_2O$

M. Durup-Ferguson,<sup>a)</sup> H. Böhlinger,<sup>b)</sup> D. W. Fahey, F. C. Fehsenfeld, and E. E. Ferguson

*Aeronomy Laboratory, National Oceanic and Atmospheric Administration, Boulder, Colorado 80303*

(Received 7 March 1984; accepted 16 May 1984)

Vibrationally excited  $O_2^+$  ions injected into a He buffered flow tube react rapidly with  $SO_2$  and  $H_2O$  by charge transfer and with  $CH_4$  to produce  $CH_3O_2^+$ ,  $CH_3^+$ , and  $CH_4^+$ . It is found that the rapidly reacting states at thermal energy are  $O_2^+(v>2)$  for  $SO_2$  and  $CH_4$  and  $O_2^+(v>3)$  for  $H_2O$ , while the lower vibrationally excited states are rapidly quenched. When the reactions of  $SO_2$  and  $CH_4$  are studied in Ar buffer as a function of kinetic energy it is found that the vibrational temperature of  $O_2^+$  established through collisional excitation by the Ar buffer is perturbed by quenching collisions with the reactant molecules. This leads to observed reaction rate constants that change with reactant gas concentration. For the reaction of  $O_2^+$  with  $CH_4$  the influence of kinetic and vibrational energy on the branching ratio of the reaction channels has been investigated. The present vibrational relaxation data for  $O_2^+(v)$  by  $CH_4$ , in conjunction with other recent measurements, allows a rather detailed picture of the mechanism to be drawn for this complicated reaction that involves the making and breaking of four chemical bonds.

## I. INTRODUCTION

A number of reactions of vibrationally excited ions have been carried out in ion swarm experiments at kinetic energies from thermal to  $\sim 1$  eV.<sup>1-4</sup> Recently, studies of vibrational relaxation of diatomic ions have been carried out in similar experiments.<sup>5-7</sup> The present measurements represent an extension of these studies to the interaction of vibrationally excited  $O_2^+$  ions with the molecules  $SO_2$ ,  $CH_4$ , and  $H_2O$ , in which competition is found between reaction and vibrational quenching channels. This competition leads to a considerable increase in the complexity of the studies.

Viehland *et al.*<sup>8</sup> have shown that the internal degrees of freedom of molecular ions drifting in atomic buffer gases can be assigned an internal temperature  $T_i$  controlled by the relative ion-buffer gas kinetic energy in steady state. Studies on several triatomic ions showed that vibrational steady state was obtained in  $\sim 10^3$  collisions with Ar buffer gas in a drift tube, but that the ions were not vibrationally excited in He buffer gas.<sup>4</sup> Direct measurement of  $O_2^+$  vibrational relaxation rate constants in He and Ar buffer gases show that  $O_2^+$  ions will attain a steady state vibrational population in Ar in experiments such as the present one involving more than  $10^3$  ion-buffer collisions and that  $O_2^+$  ions will not be vibrationally excited in He buffer gas.<sup>5,6</sup> Earlier experiments showed a large enhancement in the rate of reaction of  $O_2^+$  ions with  $CH_4$  in Ar relative to He<sup>1-3</sup> due to vibrational excitation. At that time, vibrational quenching experiments with added  $O_2$  showed directly that the  $O_2^+$  ions were vibrationally excited in Ar and not in He.<sup>2</sup>

Introducing ground state  $O_2^+$  ions into a He buffer in a flow drift tube allows rate constant measurements to be made for ground vibrational state  $O_2^+$  ions as a function of

kinetic energy. There is a large enhancement of the rate constant with kinetic energy for the exothermic reaction  $O_2^+ + CH_4^{1-3}$  and, of course, for the endothermic charge transfer of  $O_2^+$  with  $SO_2$  and  $H_2O$ . On the other hand, when a distribution of vibrationally excited  $O_2^+$  ions is injected into the flow tube, both the reaction and quenching rate constants can be determined separately for different vibrational states, using the monitor ion technique for the detection of ions in selected vibrational levels.<sup>5</sup>

In Ar buffer gas the situation is more complex. Any vibrationally excited  $O_2^+$  ions injected into an Ar buffer will be rapidly quenched, due to the large quenching rate constant  $1.0(-12)$   $cm^3 s^{-1}$  for  $O_2^+(v=1)$  and  $2.5(-12)$   $cm^3 s^{-1}$  for  $O_2^+(v=2)$ .<sup>5,6</sup> Above thermal energies, the  $O_2^+$  ions will be collisionally excited in the Ar buffer and will attain a steady state vibrational population by excitation and deexcitation in collisions with Ar. The population will be Boltzmann with a temperature  $T_i$  given by  $3/2 k_B T_i = KE_{cm}^B$ , where  $k_B$  is Boltzmann's constant and where  $KE_{cm}^B$  is the  $O_2^+$ -Ar center-of-mass kinetic energy, controlled by varying the drift tube electric field and buffer gas pressure. This would be an ideal situation for the quantitative determination of the vibrational enhancement of the rate constant except for the fact that this steady state is perturbed by the addition of the reactant gas, since  $CH_4$  is a far more effective vibrational quencher than Ar. Thus, the  $O_2^+$  vibrational temperature will depend on the  $CH_4/Ar$  ratio, i.e., the temperature will vary in the course of adding  $CH_4$  to measure the  $O_2^+ + CH_4$  rate constant. This complication was not appreciated in the earlier studies.

The present study was undertaken, in light of the recent gains in understanding, in order to see what mechanistic reaction details can be derived from competitive reaction and quenching studies. The emphasis is on the very complex  $O_2^+$  reaction with  $CH_4$ . The present results, in combination with a great wealth of other recent data on this reaction, provide a quite detailed picture of a remarkably complex reaction.

<sup>a)</sup> Permanent Address: Laboratoire de Résonance Electronique et Ionique, Université de Paris-Sud, Orsay, France.

<sup>b)</sup> Alexander v. Humboldt Foundation Scholar, permanent address: Max-Planck Institut für Kernphysik, Heidelberg, Germany.

## II. EXPERIMENTAL

The studies have been conducted in a flow-drift tube (FDT)<sup>9</sup> with a mass-selected ion source.<sup>10,11</sup> This apparatus has been used for the study of many ion-molecule reactions as a function of kinetic energy.<sup>1,2,9</sup> The basic experimental approach to studying vibrationally excited  $O_2^+$  ions in the FDT is outlined in Ref. 5. A summary of this approach is included here along with specific features of the present measurements.

Unless stated otherwise, the  $O_2^+$  primary ions in the present study have been produced in a remote electron-impact ion source. The energy of the ionizing electrons was maintained at 15.4 eV to avoid the production of metastable  $O_2^+(a^4\Pi_u)$  ions.<sup>5</sup> After mass selection, the primary ions were injected into the flow tube with the aid of a venturi inlet.<sup>10,11</sup> For He and Ne buffer gases, vibrationally excited  $O_2^+$  ions produced in the ion source were found not to be quenched in  $\sim 10^4$  collisions in the FDT.<sup>5</sup> The vibrational state distribution of the  $O_2^+$  ions in the FDT was probed by means of charge-transfer reactions with Xe,  $SO_2$ , and  $H_2O$ . The charge-transfer reactions are exothermic for  $O_2^+(v \geq 1)$ ,  $O_2^+(v \geq 2)$ , and  $O_2^+(v \geq 3)$  ions, respectively. With slight variation ( $\pm 3\%$ ), the following state distribution was found:  $O_2^+(v=0) \approx 35\%$ ,  $O_2^+(v=1) \approx 43\%$ ,  $O_2^+(v=2) \approx 11\%$ , and  $O_2^+(v \geq 3) \approx 11\%$ .

For the measurements of the ground state reaction rate constants of  $O_2^+(v=0)$  with  $SO_2$  and  $CH_4$  as a function of kinetic energy in He, the primary ions were produced by 100 eV electrons. The excited  $O_2^+$  ions were removed by adding traces of  $CO_2$  or  $O_2$  to the buffer gas. The electronically excited metastable ions of  $O_2$  react rapidly with  $CO_2$  [ $k = 9(-10) \text{ cm}^3 \text{ s}^{-1}$ ]<sup>12,13</sup> and are rapidly deexcited in collisions with  $O_2$  [ $k = 3.1(-10) \text{ cm}^3 \text{ s}^{-1}$ ].<sup>12,13</sup> The vibrationally excited ions are rapidly quenched by  $CO_2$  and  $O_2$  with rate constants of  $1(-10)$  and  $3(-10) \text{ cm}^3 \text{ s}^{-1}$ , respectively.<sup>5,6</sup>

The ions injected into the FDT were carried downstream by the fast flowing buffer gas through a field free region and into a drift region with a length of 55.9 cm. Reactant and quenching gases are added in the latter at a gas inlet port located 48.4 cm upstream of the detection system. The monitor gases for probing the vibrational state distribution of  $O_2^+$  were added at a port 3 cm upstream of the detection system. The flow tube pressure was maintained at 0.25 and 0.4 Torr with a He buffer, at 0.2 Torr with a Ne buffer, and at 0.125 and 0.2 Torr with an Ar buffer. The measurements were carried out at gas temperatures of 297 to 300 K.

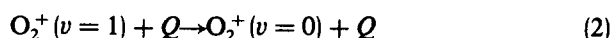
In contrast to the experiments in He and Ne buffer gases, vibrationally excited  $O_2^+$  ions are completely quenched to the ground state in an Ar buffer in the flow tube region preceding the drift-reaction region. This follows from the measured quenching rate constant<sup>5,6</sup> for Ar of  $k_q = 1(-12) \text{ cm}^3 \text{ s}^{-1}$ , the residence time of the  $O_2^+$  ions  $\tau \gg 4(-3) \text{ s}$ , and an Ar density of about  $6(15) \text{ cm}^{-3}$ .  $O_2^+(a^4\Pi_u)$  ions are destroyed even more rapidly<sup>12,13</sup> by charge transfer with the Ar buffer [ $k = 5(-10) \text{ cm}^3 \text{ s}^{-1}$ ]. At sufficiently high kinetic energy,  $O_2^+$  ions are vibrationally excited in an Ar buffer with a vibrational state distribution described by temperature  $T_i$ .<sup>8</sup> This temperature is equivalent to the mean, center-

of-mass kinetic energy in the collisions of the ions with the buffer gas atoms  $KE_{cm}^B$ :

$$\frac{3}{2} k_B T_i = KE_{cm}^B = \frac{3}{2} k_B T + \frac{1}{2} M_B v_d^2, \quad (1)$$

where  $T$  is the gas temperature,  $M_B$  is the mass of the buffer atoms, and  $v_d$  is the measured drift velocity of the ion. The theory applies when there are enough collisions of  $O_2^+$  with the buffer to reach a steady state between excitation and quenching.

The rate constant  $k_{q1}$  of the quenching process with quench gas  $Q$ :



was measured by the monitor ion technique that has been described earlier.<sup>5</sup> In these measurements, a fixed flow of Xe is added at the monitor gas inlet to convert some of the vibrationally excited  $O_2^+(v \geq 1)$  ions to  $Xe^+$  "monitor ions." The  $Xe^+$  ion signal at the detector is then proportional to the concentration of vibrationally excited  $O_2^+$  ions at the end of the FDT (except for a small contribution to the  $Xe^+$  signal from the slowly reacting ground state  $O_2^+$  ions, which is corrected for). If a quench gas is added to the FDT upstream of the monitor gas inlet, the monitor signal recorded as a function of quenching gas flow shows a decline that reflects the quenching rate constant  $k_{q1}$  (when the presence of vibrational states  $v \geq 2$  is neglected, which can be done without introducing a large error<sup>5</sup>).

In the present case of quenching by  $SO_2$ ,  $CH_4$ , and  $H_2O$ , the situation is more complex because these gases also react with the upper vibrational levels of  $O_2^+$ . For this case, the monitor ion signal recorded as a function of quenching/reactant gas addition shows a decline which reflects both the reaction rate constants of the upper vibrational levels and the quenching rate constant  $k_{q1}$  (quenching of  $v=2$  and  $v=1$  in the case of  $H_2O$ ). Thus, for the data analysis in the present study, the monitor ion technique used previously was modified. The quenching rate constant can be deduced more directly from the  $O_2^+$  signal as a function of quenching/reactant gas flow when sufficient monitor gas is added. For this case, the difference between the  $O_2^+$  signal as a function of quenching/reactant gas flow and the  $O_2^+$  signal at large flow shows a decline that closely reflects the quenching rate constant  $k_{q1}$ . With a small correction, the quenching rate constant can be deduced exactly. This procedure is explained mathematically in the Appendix.

To treat the more complex case of  $O_2^+ + CH_4$ , where there is also a nonnegligible ground state reaction, a numerical model that simulates all the reaction and quenching processes involved has been used to find the quenching rate constants by fitting the calculated results to the measured data. The model includes three different states of  $O_2^+$  with a distribution ( $v=0$ ) = 33%, ( $v=1$ ) = 45%, and ( $v \geq 2$ ) = 22%. The states of  $v=2$  and  $v > 2$  were not distinguished since they have essentially the same reaction rate coefficients with  $CH_4$ . Results of the model calculations are shown along with the corresponding experimental data in Fig. 1. Further input data for the model calculation are the fractions of ground state and excited state  $O_2^+$  ions that are converted to the monitor ion  $Xe^+$  before detection for the fixed flow of Xe gas

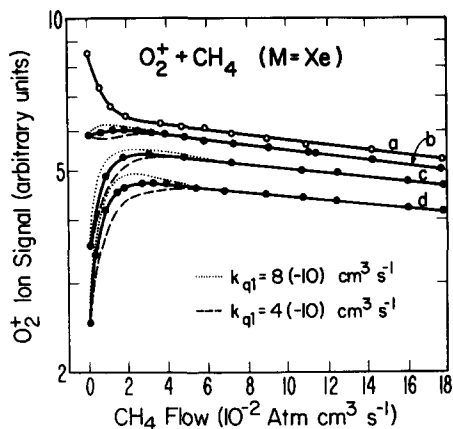


FIG. 1. Variation of the primary ion  $O_2^+$  signal as a function of quenching/reactant gas  $CH_4$  addition (points and solid curves). For (a) no monitor gas is added while (b), (c), and (d) were obtained with different constant flows of Xe monitor gas. Model calculations simulating the situation have been fitted to these data with the parameters  $k_g = 6(-12) \text{ cm}^3 \text{ s}^{-1}$ ,  $k^* = 7(-10) \text{ cm}^3 \text{ s}^{-1}$ , and a vibrational state distribution of  $(v=0) = 33\%$ ,  $(v=1) = 45\%$ , and  $(v=2) = 22\%$ . The values  $k_{q1} = 4(-10)$ ,  $6(-10)$ ,  $8(-10) \text{ cm}^3 \text{ s}^{-1}$  have been used in the calculations. The curves for  $k_{q1} = 6(-10) \text{ cm}^3 \text{ s}^{-1}$  are almost identical to the experimental data and thus are not shown.

in the measurement (these fractions are denoted  $R'$  and  $R$  in the Appendix). These two factors are determined empirically as described in Ref. 5 for each case (b), (c), and (d) shown in Fig. 1. The model calculations also give a good measure of the sensitivity of the modified monitor ion technique. The model calculations have therefore also been applied to test the  $SO_2$  and  $H_2O$  quenching results.

### III. RESULTS AND DISCUSSION

#### A. $O_2^+ + SO_2$

$SO_2$  reacts with  $O_2^+$  by charge transfer, which is exothermic by 0.19 eV for  $O_2^+$  ( $v=2$ ) and slightly endothermic by 0.039 eV for  $O_2^+$  ( $v=1$ ). As has been shown,<sup>5</sup> a fast and a slow reacting group of  $O_2^+$  ions can be distinguished experimentally in a He buffer at near thermal energy. The proportion of the two groups of ions is obtained by recording the primary ion signal as a function of reactant gas addition and extrapolating the final slope of the  $O_2^+$  signal for large flows back to zero flow in a semilogarithmic plot as indicated in Fig. 2. The fraction of fast reacting ions is designated by  $B$  and the slow reacting fraction by  $A$  in Fig. 2. The fractional abundance of the fast reacting ions in the  $O_2^+ + SO_2$  reaction is found to be  $B/(A+B) = 22\%$  at thermal energy. If the kinetic energy of  $O_2^+ - SO_2$  collisions is increased, the fraction of fast reacting  $O_2^+$  ions in a He buffer increases to 40% at 0.4 eV as shown in Fig. 3.

The rate constant that is deduced from the final slope of the  $O_2^+$  ion signal as a function of reactant gas flow (Fig. 2) will be designated by  $k_g$ , the reaction of the ground state  $O_2^+$  ions. The curve that is obtained by subtracting the straight line fitted to the final slope from the primary ion signal curve gives another rate constant that will be designated by  $k^*$  (see Fig. 4 for the example of the  $O_2^+ + CH_4$  reaction and Ref. 5).  $k^*$  corresponds to the rate of disappearance of the fast reacting ion species.

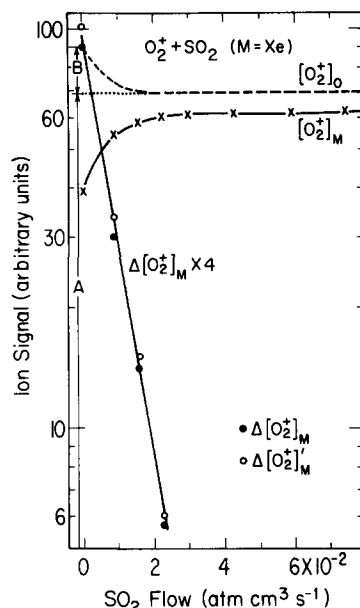


FIG. 2. Variation of the primary  $O_2^+$  ion signal as a function of quenching/reactant gas  $SO_2$  addition. Curve  $O_2^+(M)$  is with and curve  $O_2^+(0)$  without the addition of a constant flow of Xe monitor gas. Full circles show the parameter  $\Delta O_2^+(M)$  which is the difference between  $O_2^+(M)$  and  $O_2^+(M)$  when  $[SO_2] = \infty$ . Open circles are the corrected values  $\Delta O_2^+(M)'$  (see the Appendix). The quenching rate constant  $k_{q1}$  ( $SO_2$ ) is deduced from the linear decline of  $\Delta O_2^+(M)'$ .

At thermal energy, a rate constant  $k^*$  of  $1.2(-9) \text{ cm}^3 \text{ s}^{-1}$  is determined.<sup>5</sup>  $k^*$  is the sum of the reaction rate constant  $k_2$  and the quenching rate constant  $k_{q2}$  for the  $O_2^+$  ( $v \geq 2$ ) ions.<sup>5,13</sup> Unfortunately, the two rate constants cannot be determined independently. If one assumes that the vibrational distribution of the  $O_2^+$  ions given by the Franck-Condon factors<sup>14</sup> is an upper limit to the vibrational excitation in the present experiment, one obtains  $O_2^+$  ( $v \geq 2$ )  $< 45\%$  and  $k_2 \geq k_{q2}$ .  $k^*$  was found to be constant in the energy range from thermal energy to 0.2 eV.

The reaction rate constant of the charge transfer of  $O_2^+$  ( $v=0$ ) with  $SO_2$  as a function of kinetic energy has been measured and the results are shown in Fig. 5. The rate constant is steeply increasing with energy as expected for an endothermic reaction. At energies below 0.1 eV,  $O_2^+$  associates with  $SO_2$  and therefore no values for the charge transfer reaction rate constant are given for this energy range.

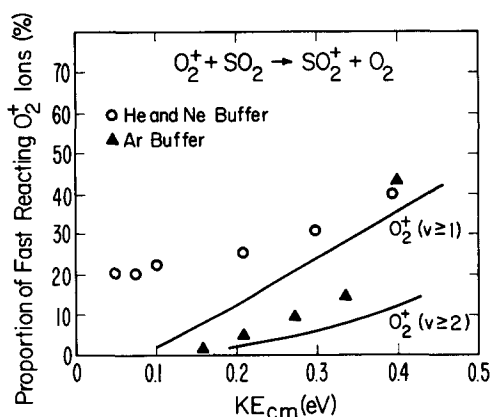


FIG. 3. Fraction of  $O_2^+(v)$  ions reacting fast with  $SO_2$  as a function of relative kinetic energy with respect to ion-reactant collisions  $KE_{cm}^R$ , in He, Ne, and Ar buffers. In He and Ne buffers the  $O_2^+$  ions have the vibrational state distribution they attained prior to injection (see the text) while in the Ar buffer the excitation is determined by collisions with the buffer. The vibrational state distribution calculated for the  $O_2^+$  ions in the Ar buffer at excitation and deexcitation steady state (solid lines) is shown for comparison.

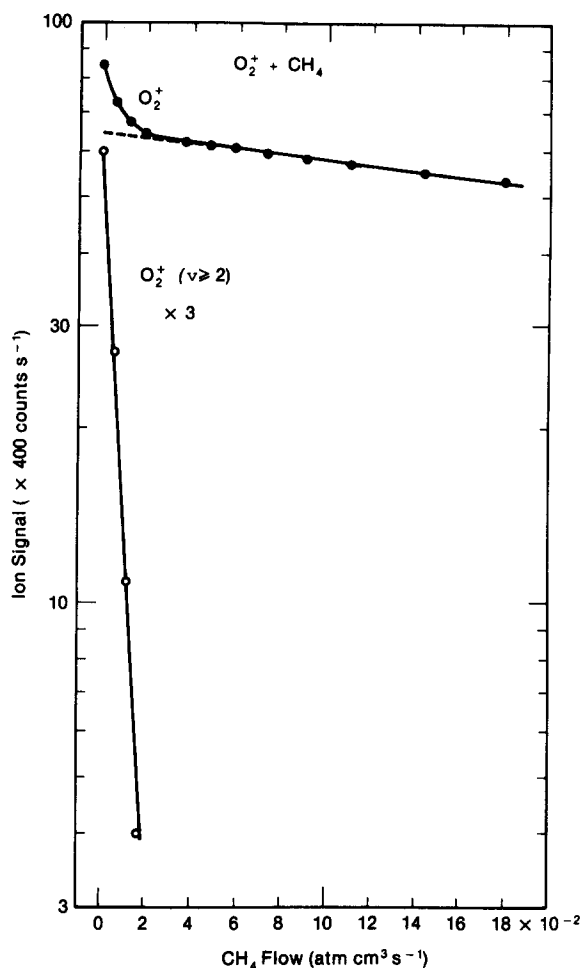


FIG. 4. Reaction of  $CH_4$  with  $O_2^+$  ions in the given vibrational state distribution in the He buffer at near thermal energy. The dashed line gives the ground state rate constant  $k_g$ , while the steep straight line gives  $k^*$  for  $O_2^+$  ( $v \geq 2$ ).

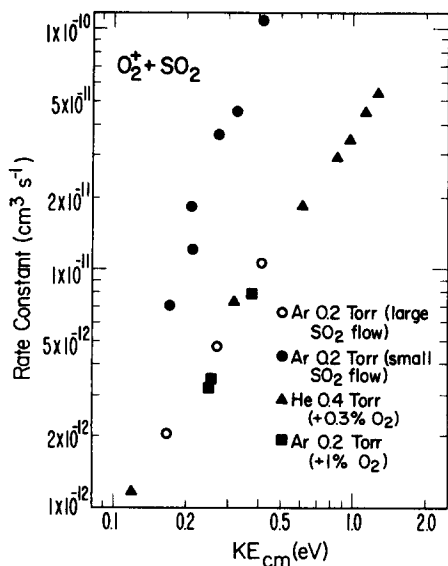


FIG. 5. Rate constant of the reaction  $O_2^+ + SO_2$  as a function of kinetic energy in He and Ar buffers. In He the reactant ions are only  $O_2^+$  ( $v = 0$ ) due to quenching by  $CO_2$ . In the Ar buffer at energies above the threshold for vibrational excitation ( $\sim 0.12$  eV) two reaction rate constants for the limiting conditions of very small and very large  $SO_2$  flows are given (see  $k_a$  and  $k_b$  in Fig. 9, respectively).

The quenching rate constant  $k_{q1}$  of  $O_2^+$  ( $v = 1$ ) by  $SO_2$  has been measured at near thermal energy by the modified monitor ion technique using Xe as monitor gas. The result of the measurement is shown in Fig. 2. A quenching rate constant of  $k_{q1} = 5.7(-10)$   $cm^3 s^{-1}$  has been deduced from these data.

The results in Fig. 3 can now be explained in the following way: The fast reacting species at thermal energy are mostly  $O_2^+$  ( $v \geq 2$ ) ions. The endothermic charge transfer reaction of  $O_2^+$  ( $v = 1$ ) is certainly slower at thermal energy than the quenching and contributes only to a very small degree to the observed rapidly reacting ions. In a similar case, the endothermic charge transfer reaction of  $O_2^+$  ( $v = 0$ ) + Xe ( $\Delta H = +0.06$  eV) has a reaction rate constant of  $6(-11)$   $cm^3 s^{-1}$  at thermal energy.<sup>5</sup> When the kinetic energy is increased, however, the quenching rate constant  $k_{q1}$  is expected to decrease while the reaction rate constant for  $O_2^+$  ( $v = 1$ ) increases, which results in an increasing fraction of  $O_2^+$  ( $v = 1$ ) ions that contribute to the fast reacting species as shown in Fig. 3.

In an Ar buffer at energies above 0.15 eV, the  $O_2^+$  ion signal does not decline exponentially as a function of  $SO_2$  flow. Instead, a curvature is observed on a semilogarithmic plot at low flows and a straight line observed only for large reactant gas flows. The rate constant that corresponds to this final exponential decline is exactly the same as the ground state rate constant for the same kinetic energy. This indicates that for these large reactant gas flows (0.5%–3% of the buffer flow) the vibrationally excited ions are more rapidly depleted by quenching and reaction than the vibrational state distribution can be reestablished by collisional excitation. This effect will be discussed in more detail for the  $O_2^+ + CH_4$  reaction. The rate constants in an Ar buffer for the final decline of the primary ion signal and for the limiting case, of very small  $SO_2$  flow (designated  $k_b$  and  $k_a$ , respectively, for the case of  $O_2^+ + CH_4$ ) are given in Fig. 5 as a function of kinetic energy. The rate constant  $k_a$  for very small  $SO_2$  flows should be the rate constant averaged over a vibrational state distribution given by the temperature  $T_i$  since the excitation of  $O_2^+$  is mostly determined by collisions with the Ar buffer.

If the final exponential decline is extrapolated back to zero flow, one obtains the ratio of fast and slow reacting ions similar to the case in a He buffer. The fraction of fast reacting ions is given as a function of kinetic energy in Fig. 3. Also shown are the fractions of  $O_2^+$  ions that are expected to be in the vibrationally excited states  $v \geq 1$  and  $v \geq 2$  for the given internal temperature  $T_i$ , assuming a Boltzmann distribution. One expects that the fraction of fast reacting ions is roughly proportional to the concentration of the excited states of  $O_2^+$  that can react fast. The proportionality factor depends on the rate at which the excited states can be repopulated. Small deviations from proportionality are expected because the residence time and the excitation rate change with kinetic energy. Figure 3 shows that the fraction of fast reacting ions follows the curve for the fraction of  $O_2^+$  ( $v \geq 2$ ) ions for low kinetic energy. This is consistent with the results in a He buffer at near thermal energy where only  $O_2^+$  ( $v \geq 2$ ) ions were found to react rapidly. At an energy of 0.3–0.4 eV,

TABLE I. Measured reaction rate constants of the fast reacting  $O_2^+$  species  $k^*$ , the ground state  $O_2^+$  ions  $k_g$ , the fraction of fast reacting  $O_2^+$  ions  $B/A + B$ , quenching rate constants for  $O_2^+(v=1)$   $k_{q1}$ , and collision rate constants  $k_c$  for the ion-neutral pair at thermal energy.

Reactant neutral	$k^*$ [ $\text{cm}^3 \text{s}^{-1}$ ]	$k_g$	$B/A + B$	$k_{q1}$	$k_c$
$\text{SO}_2$	1.2(-9) <sup>a</sup>	<1(-12)	0.22	5.7(-10)	1.2(-9) <sup>b</sup>
$\text{H}_2\text{O}$	1.35(-9)	<1(-12)	0.11	1.2(-9)	1.4(-9)
$\text{CH}_4$	7(-10)	5(-12)	0.25	6(-10)	1.14(-9)

<sup>a</sup> $a(-b) = a \times 10^{-b}$ .

<sup>b</sup>See Ref. 5 for calculation of  $k_c$ .

a transition is observed indicating that  $O_2^+(v=1)$  ions also begin to react rapidly. This is probably a consequence of the fact that, at energies above about 0.35 eV,  $O_2^+(v=1)$  reacts faster than it is quenched by  $\text{SO}_2$ .

The fact that vibrationally relaxed  $O_2^+$  ions (with large  $\text{SO}_2$  flow) have the same charge-transfer rate constant with  $\text{SO}_2$  as  $O_2^+$  ions in He proves that there is no rotational enhancement of the charge-transfer rate constant since the rotational temperature is very much higher in the Ar than in the He buffer. This result was found earlier for  $\text{N}_2\text{O}^+$  charge transfer with  $\text{NO}$ .<sup>4</sup>

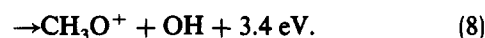
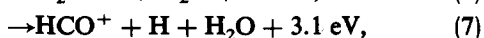
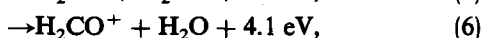
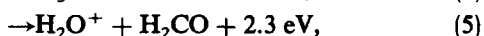
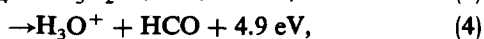
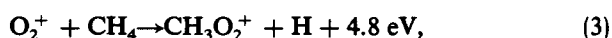
The rate coefficients measured at thermal energy for this system are summarized in Table I. The uncertainties in the measurements are estimated to be the following:  $k_g$  was measured with the standard accuracy of the technique ( $\pm 30\%$ ). The accuracy was estimated to be (+60%/-40%) for  $k^*$  and  $k_b$ , (+80%/-50%) for  $k_a$ , and (+75%/-40%)<sup>5</sup> for  $k_{q1}$ .

## B. $O_2^+ + \text{H}_2\text{O}$

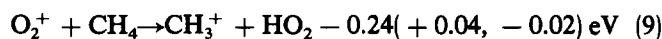
$\text{H}_2\text{O}$  reacts exothermically only with  $O_2^+(v \geq 3)$  ions by charge transfer. 11%  $\pm$  2% of the  $O_2^+$  ions in the given state distribution in the FDT have been found to react fast with a rate constant  $k^*$  of 1.35(-9)  $\text{cm}^3 \text{s}^{-1}$ . The quenching rate constant for  $O_2^+(v=1)$  by  $\text{H}_2\text{O}$  has been determined by the  $\text{Xe}^+$  monitor ion technique to be  $k_{q1} = 1.2(-9) \text{cm}^3 \text{s}^{-1}$ .

## C. $O_2^+ + \text{CH}_4$

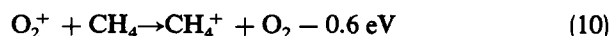
In this reaction, three different channels are observed, two of them are endothermic for  $O_2^+(v=0)$  and become exothermic for  $O_2^+(v=2)$  and  $O_2^+(v=3)$ . This, added to the fact that the quenching rate constant of  $O_2^+(v \geq 1)$  by  $\text{CH}_4$  is one-half Langevin,<sup>5</sup> makes it a very complicated reaction and, at the same time, a good candidate for the study of competition between reactive and quenching collisional processes. Among six possible exothermic channels only reaction (3) is observed, leading to the formation of the  $\text{CH}_3\text{O}_2^+$  ion



Two endothermic product channels for  $O_2^+(v=0)$  are also observed:



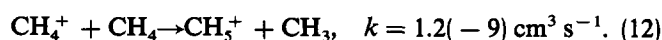
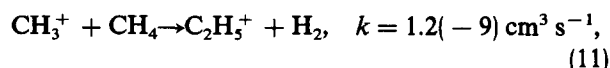
which becomes exothermic by 0.22 eV for  $O_2^+(v=2)$  and



which is exothermic by 0.09 eV for  $O_2^+(v=3)$ .

The thermochemical data are taken from Refs. 15-17 and the heat of formation of  $\text{HO}_2$  from Ref. 18.

The product ions  $\text{CH}_3^+$  and  $\text{CH}_4^+$  react rapidly with  $\text{CH}_4$ ,<sup>19</sup>



$\text{CH}_3^+$  and  $\text{CH}_4^+$  are therefore only intermediate species with very small abundances and their production is monitored by the ion signals of  $\text{C}_2\text{H}_5^+$  and  $\text{CH}_5^+$ .

The structure of the product ion  $\text{CH}_3\text{O}_2^+$  is protonated formic acid, i.e.,  $\text{HC}(\text{OH})_2^+$ , whose heat of formation<sup>17</sup> is 97.2 kcal mol<sup>-1</sup>. The structure has been established by Lindinger and his colleagues<sup>20,21</sup> in two different kinds of experiments. Isotopic exchange with  $\text{D}_2\text{O}$  has been measured for the  $\text{CH}_3\text{O}_2^+$  product of reaction (3) and for  $\text{CH}_3\text{O}_2^+$  produced by reaction of formic acid ion with formic acid with identical results, namely the two OH hydrogen atoms are successively exchanged while the CH hydrogen is not.<sup>20</sup> Also, collisional breakup of the  $\text{CH}_3\text{O}_2^+$  ions produced both ways gives identical results<sup>21</sup>; the ions  $\text{H}_3\text{O}^+$  and  $\text{HCO}^+$  are produced in comparable abundance at all kinetic energies sufficient for breakup.

The energy dependence of the individual rate constants of the reaction channels (3), (9), and (10) and of the overall reaction rate constant for  $O_2^+(v=0)$  ions in He buffer is shown in Fig. 6. These measurements were performed using the electron impact ion source immersed in the flow tube and adding enough  $\text{O}_2$  so that all primary ions were quenched to the ground vibrational state by  $O_2^+ - \text{O}_2$  collisions. The measurements were also repeated with the mass-selected ion

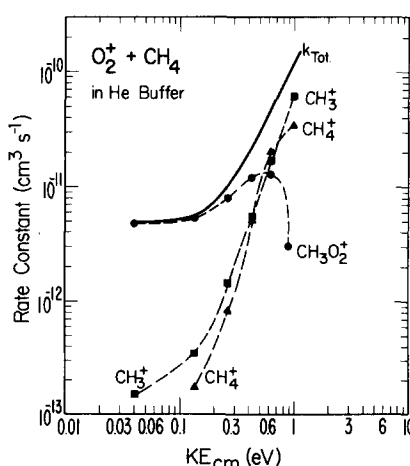


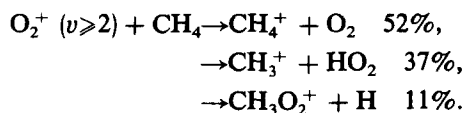
FIG. 6. Rate constants for the three individual reaction channels in the reaction of  $O_2^+(v=0)$  with  $\text{CH}_4$  as a function of kinetic energy in the He buffer.

source and the contribution of the fast reacting excited ion species to the three product channels was subtracted from the ion signals. The results of both measurements were identical.

Figure 6 shows that the steep increase of the reaction rate constant for  $O_2^+ (v=0) + CH_4$  above about 0.15 eV is mainly due to the opening of the two endothermic reaction channels (9) and (10). The small  $CH_3^+$  and  $CH_4^+$  signals at low energy are consistent with the endothermicities of reaction channels (9) and (10). The  $CH_3^+$  signal at 0.04 eV ( $3/2 k_B T$ ) corresponds to a rate constant  $\sim 1(-13) \text{ cm}^3 \text{ s}^{-1}$ , about  $10^{-4}$  of the collision rate constant. The Boltzmann factor  $\exp(-0.24/k_B T)$  is also near  $10^{-4}$ . The  $CH_4^+$  channel has an equivalent  $1(-13) \text{ cm}^3 \text{ s}^{-1}$  rate constant near 0.1 eV, or 2.5 times higher than the  $CH_3^+$  value, corresponding to the  $\sim 2.5$  time greater activation energy, or  $\sim 0.6$  eV.

When the  $O_2^+$  ions in the given vibrational state distribution (65% in  $v \geq 1$ , 22% in  $v \geq 2$ , and 11% in  $v \geq 3$ ) produced in the mass selected ion source are reacted with  $CH_4$ , one observes that  $\sim 24 \pm 2\%$  of the  $O_2^+$  ions undergo a very rapid reaction, as shown in Fig. 4, with a rate constant  $k^* = 7(-10) \text{ cm}^3 \text{ s}^{-1}$ . This fraction, almost identical to that reacting rapidly with  $SO_2$ , must be almost exclusively the  $O_2^+$  ions in  $v \geq 2$ . The reaction rate constant of the slowly reacting ions is identical to the rate constant for  $O_2^+ (v=0)$  ions,  $k_g = 5(-12) \text{ cm}^3 \text{ s}^{-1}$  obtained from measurements where the  $O_2^+$  ions were vibrationally relaxed by  $O_2$  collisions prior to the reaction. This is already an indication that the population of  $O_2^+ (v=1)$  is very rapidly relaxed by  $CH_4$ .

The branching ratio of the three reaction channels for the fast reacting ions can be determined from the results shown in Fig. 7:



From these percentages, one can calculate that for the whole population of  $O_2^+$  ions,  $12.5 \pm 2\%$  react to give  $CH_4^+$ . For this reaction channel,  $O_2^+ (v \geq 3)$  are required, the abundance of which is about 11%. This leads to the conclusion that all the  $O_2^+ (v \geq 3)$  ions react by charge transfer with  $CH_4$ . The  $11.5 \pm 2\%$  of the whole population of  $O_2^+$  given  $CH_3^+$  and  $CH_3O_2^+$  are therefore all the  $O_2^+$  in  $v=2$ .

The absence of the contribution of  $O_2^+ (v=1)$  to the endothermic production of  $CH_3^+$  is consistent with the fact that the  $O_2^+ (v=1)$  are more rapidly quenched than they react at thermal energy. This is shown by the results in Fig. 1 obtained with the  $Xe^+$  monitor ion technique. The recovery of the  $O_2^+$  ion signal with  $CH_4$  gas flow at a fixed monitor gas flow indicates that the current of ground state ions reaching the monitor gas inlet increases. The quenching rate constant  $k_{q1}$  obtained from fitting model calculations to the measured results is  $6(-10) \text{ cm}^3 \text{ s}^{-1}$ .

When, in a different experimental approach, the products  $CH_3^+$  and  $CH_4^+$  from the  $O_2^+ + CH_4$  reaction were used as monitor ions to study the quenching of vibrationally excited  $O_2^+$  ions with  $CO_2$  and Kr, the values  $k_q(CO_2) = 2.1(-10) \text{ cm}^3 \text{ s}^{-1}$  and  $k_q(Kr) = 1.6(-11)$

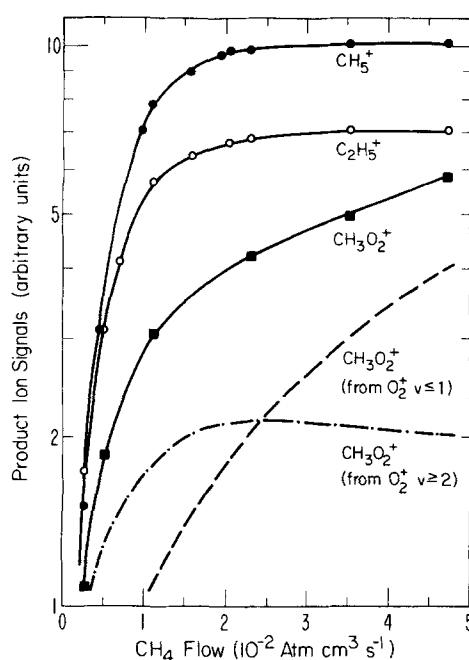


FIG. 7. Ion signals of the product ions from reaction  $O_2^+ (v) + CH_4$  as a function of  $CH_4$  flow in the He buffer. The curve  $CH_3O_2^+$  [from  $O_2^+ (v < 1)$ ] is calculated from the known ground state reaction rate constant  $k_g$  and the relative concentration of  $O_2^+ (v=0,1)$  ions. The curve  $CH_3O_2^+$  [from  $O_2^+ (v \geq 2)$ ] is obtained by subtraction of  $CH_3O_2^+$  from  $O_2^+ (v < 1)$  from the total  $CH_3O_2^+$  curve. The branching ratio of the three product channels  $CH_3^+$ ,  $CH_4^+$ , and  $CH_3O_2^+$  in the reaction  $O_2^+ (v \geq 2) + CH_4$  is obtained from these data.

$10^{-11} \text{ cm}^3 \text{ s}^{-1}$  were obtained. The values were thus almost identical for both monitor ions. These values are in very good agreement with the results obtained<sup>5,6</sup> with the  $SO_2^+$  monitor ion technique  $k_{q2}(CO_2) = 2(-10) \text{ cm}^3 \text{ s}^{-1}$  and  $k_{q2}(Kr) = 1.7(-11) \text{ cm}^3 \text{ s}^{-1}$ . This confirms the conclusion that at room temperature the product ions  $CH_3^+$  and  $CH_4^+$  are primarily due to  $O_2^+ (v \geq 2)$  ions. One would expect that the quenching rate constant observed with the  $CH_4^+$  monitor ions would be higher than  $k_{q2}$  because it should essentially give  $k_{q3}$ , but the experimental technique may not be accurate enough to resolve the small difference between  $k_{q2}$  and  $k_{q3}$  in this case.

Figure 8 summarizes the results of reaction rate constant measurements as a function of kinetic energy in the different buffer gases He, Ne, and Ar. In a Ne buffer, about 24% of the  $O_2^+$  ions reacted rapidly just as in the case of a He buffer, indicating that the vibrationally excited ions produced in the ion source are not quenched in the FDT in agreement with the earlier observations.<sup>5,6</sup> The rate constants given for He and Ne buffer gases are those of the slowly reacting ground state  $O_2^+$  ions. The rate constants in He and Ne are identical within the experimental error limit over the entire energy range. This implies that the  $O_2^+$  ions are not vibrationally excited in Ne. This differs from the observations of Alge *et al.*<sup>3</sup> who found a rate constant enhancement in Ne. In order to further demonstrate that there is no significant excitation of  $O_2^+$  in Ne buffer at high kinetic energy in the FDT, 2% of  $O_2$  gas was added to the buffer which should result in a very efficient quenching of vibrational excitation. No change in the rate constant of the slowly react-

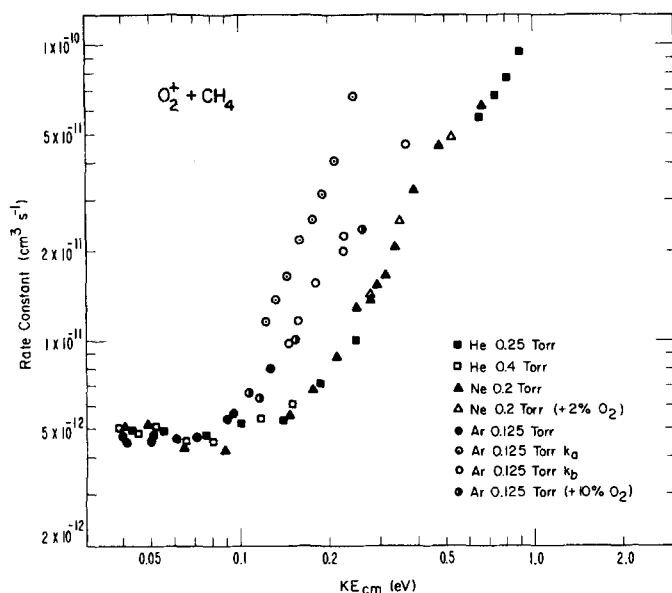


FIG. 8. Rate constant of the reaction  $O_2^+ + CH_4$  as a function of kinetic energy in He, Ne, and Ar buffers. The reaction rate constants in pure He and Ne buffers are those for the ground state ion  $k_g$ . For the Ar buffer at energies above the threshold for vibrational excitation of  $O_2^+$  ( $\sim 0.12$  eV), two rate constants  $k_a$  and  $k_b$ , for small and large  $CH_4$  flows, have been determined (see Fig. 9). In some measurements in the Ne and Ar buffers,  $O_2$  has been added to quench the vibrational excitation of the  $O_2^+$  ions.

ing ions was observed while the fast reacting ions disappeared.

In an Ar buffer, where excitation of the  $O_2^+$  ions in the FDT is possible at sufficiently high kinetic energy, a curvature appears above 0.12 eV in the decline of the logarithm of the ion signal as a function of  $CH_4$  flow. A typical example of a measurement at 0.23 eV is shown in Fig. 9 (the reaction rate constants given in Fig. 8 for Ar buffer at  $KE_{cm} > 0.12$  eV are those for the limiting cases of very small and very large flows of  $CH_4$ ,  $k_a$ , and  $k_b$ , respectively). The observation of a change in the slope of the decline is similar to the behavior of the reaction  $O_2^+ + SO_2$  in an Ar buffer. The two cases differ

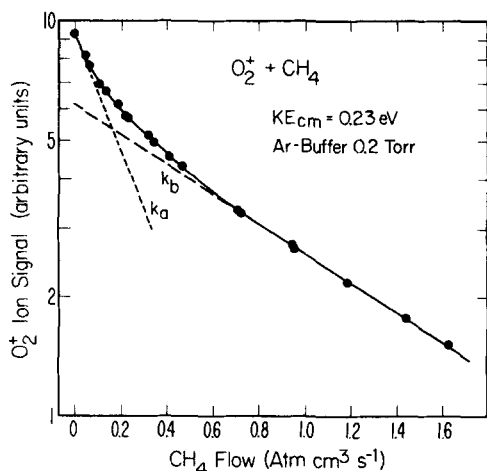
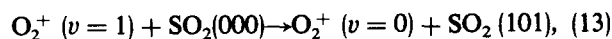


FIG. 9. Typical result in the measurement of the rate constants for the reaction  $O_2^+ + CH_4$  in the Ar buffer at energies above the threshold for vibrational excitation of  $O_2^+$  ( $\sim 0.12$  eV). No unique rate constant can be obtained but rate constants for the limiting conditions of very small and very large  $CH_4$  flows,  $k_a$  and  $k_b$ , respectively, have been deduced.

however. For  $O_2^+ + SO_2$ , the rate constant for large  $SO_2$  flow coincides with the ground state rate constant measured in He buffer while for  $O_2^+ + CH_4$  the rate constants for large  $CH_4$  flow in Ar is still significantly higher than the ground state rate constant. When 10%  $O_2$  gas is added to the Ar buffer to quench the vibrationally excited  $O_2^+$  ions, the curvature in the primary ion decay disappears for the reaction  $O_2^+ + CH_4$  and the unique rate constant derived is identical to that for large  $CH_4$  flows (as shown in Fig. 8).

The change of the reactivity of  $O_2^+$  as a function of reactant gas addition in the case of the reactions  $O_2^+ + SO_2$  and  $O_2^+ + CH_4$  in an Ar buffer at high kinetic energy can be understood in the following way: The quenching rate constants measured for the deactivation of  $O_2^+*$  by  $SO_2$  and  $CH_4$  are about  $k_{q1} = 6(-10)$   $cm^3 s^{-1}$  while the quenching rate constant for Ar is only  $1(-12)$   $cm^3 s^{-1}$  at thermal energy.<sup>5,6</sup> From detailed balance, one expects that the excitation rate constants have the same order of magnitude at kinetic energies above the excitation threshold as the quenching rate constants. More precisely, both rate constants should decrease somewhat with increasing kinetic energy (not more than an order of magnitude) as expected from the quenching studies.<sup>5,6</sup> Since relaxation and excitation by  $CH_4$  and  $SO_2$  is about 600 times faster than by the Ar buffer, one expects that the internal temperature of the  $O_2^+$  ions in the FDT is controlled almost exclusively by the collisions with  $CH_4$  and  $SO_2$  when these gases are added to the buffer in mixing ratios larger than 1%. In the case of  $CH_4$ , the internal temperature of  $O_2^+$  is expected to decrease because of the light mass of  $CH_4$  compared to Ar and also because of the ability of the buffer to store internal energy. Inelastic collisions resulting in excitation transfer to the buffer have been found by Viehland and Fahey<sup>22</sup> to lower the kinetic energy of the ions and, similarly, one expects that the internal energy of the molecular ion is decreased compared to the value calculated from Eq. (1). It is surprising, that for large  $SO_2$  addition, the  $O_2^+$  ions show a reactivity as if they were all quenched to the ground state. For the large mass of  $SO_2$  one would expect a larger degree of excitation than for the case of  $CH_4$ . One possible explanation is that V-V transfer occurs in this case so that detailed balancing does not apply under drift tube conditions, i.e., vibrational deexcitation is much faster than excitation. For example, the two quantum excitations of  $SO_2$ ,



must be nearly resonant, since  $h\nu[SO_2(100)] + h\nu[SO_2(001)] - h\nu[O_2^+ (v = 1)] = 9$   $cm^{-1}$ .

Small differences in the rate constants of ion-molecule reactions in different buffer gases can occur due to differing speed distributions of the drifting primary ions. This has been demonstrated<sup>23</sup> for the reaction  $O^+ + N_2$  which shows an extremely steep increase of the rate constant with kinetic energy. For the reaction  $O_2^+ + Xe$ <sup>5,6</sup> and also for  $O_2^+ + SO_2$  with large addition of  $SO_2$ , no differences are observed in the rate constants obtained in He and Ar buffer gases. Therefore, one does not expect that the difference in speed distributions causes a significant effect in the reaction  $O_2^+$



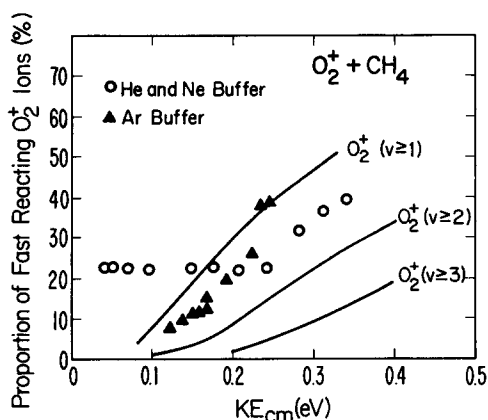
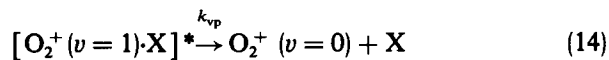


FIG. 10. Fraction of  $O_2^+(v)$  ions reacting fast with  $CH_4$  as a function of the ion-reactant center-of-mass kinetic energy  $KE_{cm}^R$ , in He, Ne, and Ar buffer gases. In He and Ne, the vibrational state distribution of the  $O_2^+$  ions is equal to that prior to injection into the flow tube (see the text). In an Ar buffer, the vibrational state distribution is determined by exciting and de-exciting collisions of  $O_2^+$  with the buffer. The distribution calculated for steady state is shown in the figure for comparison.

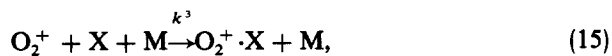
+  $CH_4$ , which shows less variability of the rate constant with energy than the reaction  $O^+ + N_2$ .

The fraction of  $O_2^+$  ions reacting fast with  $CH_4$  in an Ar buffer can be found in the same way as for the  $SO_2$  reaction. Figure 10 shows the percentage of rapidly reacting  $O_2^+$  as a function of kinetic energy along with the fractions of  $O_2^+$  ions expected to be in the excited states  $O_2^+(v > 1)$ ,  $O_2^+(v > 2)$ , and  $O_2^+(v > 3)$  for the corresponding excitation temperature  $T_i$ . The data indicate that below 0.25 eV the fast reacting ions are mainly  $O_2^+(v > 2)$  ions while above 0.25 eV,  $O_2^+(v = 1)$  ions also react rapidly.

The present vibrational quenching data combined with other recent data on the  $O_2^+ + CH_4$  reaction, yield a rather detailed picture of the reaction mechanism. The vibrational quenching rate constant  $k_{q1} = 6(-10) \text{ cm}^3 \text{ s}^{-1}$  allows an estimate of the  $[O_2^+ \cdot CH_4]^*$  collision complex lifetime. The rate of vibrational predissociation of the complexes



are found to be  $k_{vp} \sim 10^9 \text{ s}^{-1}$  for  $X = \text{Ar}, N_2, CO_2, H_2O$ , and  $SO_2$  and for  $NO^+(v)$  vibrational predissociation by  $CO_2, CH_4, NH_3$ , and  $CO$ .<sup>24,25</sup> These values are derived from the expression  $k_{vp} = k_q k_s / k^3$ , where  $k_q$  is the experimental vibrational quenching rate constant,  $k^3$  is the experimental three-body association rate constant for



and  $k_s$  is the stabilization rate constant for



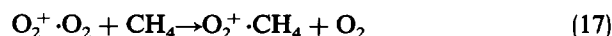
assumed to be the collision rate constant  $k_s = k_c = 2\pi e(\alpha/\mu)^{1/2}$  for heavy  $M \neq \text{He}$ . The relation  $k_{vp} = k_q k_s / k^3$  is valid for the cases where vibrational quenching is slow, i.e.,  $k_q < k_c$ , otherwise vibrational quenching is rate limited by the complex formation step and the derived value of  $k_{vp}$  is only a lower limit. Since  $O_2^+(v=1)$  is quenched in about

half the collisions with  $CH_4$  (Table I), it appears that the complex lifetime is comparable to the reciprocal vibrational predissociation rate  $k_{vp}^{-1} \sim 1(-9) \text{ s}$ . This is a longer lifetime than one would expect from purely electrostatic bond considerations. For example, the lifetime  $\tau$  of the  $NO^+ \cdot CH_4$  complex can be estimated to be  $\sim 3(-11) \text{ s}$  at 300 K from  $k^3 = k_1 k_s \tau$ . The complex formation rate constant and the collisional stabilization rate constant are assumed to be Langevin and the  $NO^+ + CH_4 + M \rightarrow NO^+ \cdot CH_4$  three-body rate constant<sup>26</sup> is  $k^3 < 2(-29) \text{ cm}^6 \text{ s}^{-1}$  in a  $\text{He}/N_2 = 2.25$  gas mixture at 300 K.

The mechanism leading to a longer lifetime for  $O_2^+ \cdot CH_4$  complex is believed to be  $H^-$  abstraction to form  $CH_3^+ \cdot HO_2$  in the complex. This is the 0.24 eV endothermic reaction (4) except that the  $HO_2$  (with a very large dipole moment of 2 D) is trapped and cannot separate at thermal energy. The electrostatic attraction energy is quite enough to supply this 0.24 eV at impact. This is analogous to the situation recently described in which  $Si^+$  was found to have an anomalously large three-body association with  $O_2$  by virtue of the slightly endothermic formation of  $SiO^+ \dots O$  complex which allows  $Si^+$  access to the deep potential well between the oxygen atoms.<sup>27</sup> That hydride ion ( $H^-$ ) abstraction occurs is evident from the steep onset of  $CH_3^+$  production at threshold shown in Fig. 6. Hydride ion abstractions as a class are very often efficient so this is not an unexpected result. The hydride ion abstraction first step in reaction (3) aids greatly in terms of reaction dynamics as well. The reaction of  $O_2^+$  with  $CH_4$  to produce protonated formic acid is a remarkable one, involving the breaking of the O-O bond and three C-H bonds with the formation of two C-O and two O-H bonds. The initial  $H^-$  abstraction lowers the O-O bond strength from 6.7 eV in  $O_2^+$  to 2.6 eV in  $HO_2$ , as well as breaking one C-H bond and making one O-H bond. Since the reaction probability for reaction (3) is  $\sim 5(-3)$ , the ratio of  $k_g$  to  $k_c$  in Table I, the lifetime of the  $[O_2^+ \cdot CH_4]^*$  (or  $[CH_3^+ \cdot HO_2]^*$ ) complex against reaction to produce  $CH_3O_2^+ + H$ , must be  $\sim \tau/P \sim 5(-10)/5(-3) \sim 1(-7) \text{ s}$ .

A recent experiment which beautifully confirms this picture is the measurement of reaction (3) down to 20 K in a uniform supersonic jet at Meudon, and confirmed down to 70 K by flow-drift tube measurements at Birmingham.<sup>28</sup> The value of  $k_g$  increases with decreasing temperature, following a very linear  $T^{-1.8}$  dependence from  $\sim 150$  down to 20 K. At 20 K the rate constant is  $5(-10) \text{ cm}^3 \text{ s}^{-1}$ , almost half of  $k_c = 1.14(-9) \text{ cm}^3 \text{ s}^{-1}$ . A smooth extrapolation on a linear  $T$  scale yields almost exactly  $k_c$  at 0 K. This is qualitatively quite consistent. The lifetime will increase with decreasing  $T$  and at 20 K will be  $\tau(20 \text{ K}) \sim \tau(300 \text{ K}) (\frac{300}{20})^{1.8} \approx 1(-7) \text{ s}$ . This is comparable to the lifetime for  $CH_3O_2^+$  production [i.e., reaction (3)] so that reaction should occur on  $\sim 1/2$  the collisions as observed.

An interesting observation is that the reaction



has been observed,<sup>29,30</sup> i.e., a stable  $O_2^+ \cdot CH_4$  cluster ion exists in spite of the fact that  $O_2^+$  reacts with  $CH_4$ . However, the reaction scheme we have suggested above requires that the  $O_2^+$  and  $CH_4$  collide with the 0.24 eV energy necessary

for hydride ion abstraction by the O<sub>2</sub><sup>+</sup>. Evidently when the CH<sub>4</sub> is “gently” inserted in the switching reaction (17), the endothermic hydride ion abstraction cannot occur and therefore the subsequent CH<sub>3</sub>O<sub>2</sub><sup>+</sup> production on ~1(–7) s time scale also does not occur.

#### IV. SUMMARY AND CONCLUSIONS

For the reactions O<sub>2</sub><sup>+</sup> + SO<sub>2</sub>, O<sub>2</sub><sup>+</sup> + CH<sub>4</sub>, and O<sub>2</sub><sup>+</sup> + H<sub>2</sub>O, very fast quenching of the first vibrationally excited state of O<sub>2</sub><sup>+</sup> was found while reaction of this state was very slow at thermal energy. Only at higher kinetic energy does the reactive channel become dominant in the reactions of O<sub>2</sub><sup>+</sup> (*v* = 1) with SO<sub>2</sub> and CH<sub>4</sub>. In the absence of reaction, one would expect that the vibrational states O<sub>2</sub><sup>+</sup> (*v* = 2) and O<sub>2</sub><sup>+</sup> (*v* = 3) would be even more efficiently quenched by SO<sub>2</sub> or CH<sub>4</sub> than is O<sub>2</sub><sup>+</sup> (*v* = 1). For the higher vibrational levels however, the quenching process is in competition with exothermic reaction channels. For these states it is observed that reactive processes occur at almost the collision rate and dominate the quenching.

In the reaction O<sub>2</sub><sup>+</sup> + CH<sub>4</sub>, the two endothermic reaction channels leading to CH<sub>3</sub><sup>+</sup> and CH<sub>4</sub><sup>+</sup> become dominant at higher kinetic energy (≥0.5 eV) and at higher internal energy (*v* > 2) of the O<sub>2</sub><sup>+</sup> ions. Quite similar observations have been made by Tanaka *et al.*<sup>31</sup> who used an experimental technique in which the O<sub>2</sub><sup>+</sup> ions can be prepared in the selected vibrational states *v* = 0, 1, and 2.

In the reaction studies in an Ar buffer at higher kinetic energies, the steady state of vibrational excitation and deexcitation of O<sub>2</sub><sup>+</sup> is mainly controlled by the reactant gases CH<sub>4</sub> and SO<sub>2</sub> when they are added to the buffer in quantities larger than a few tenths of a percent. It is not possible to predict the steady-state internal temperature of O<sub>2</sub><sup>+</sup> in this case because *T<sub>i</sub>* depends on the degree to which collisional energy and vibrational energy of O<sub>2</sub><sup>+</sup> are transferred into the internal modes of the molecular targets during collisions.

The combination of the present O<sub>2</sub><sup>+</sup>(*v*) vibrational quenching and reaction studies with CH<sub>4</sub>, recent very low temperature measurements of the reaction rate constant, and collisional breakup studies and isotopic exchange studies of the CH<sub>3</sub>O<sub>2</sub><sup>+</sup> product ion, allow a rather detailed insight into the reaction mechanism. This also involves the recently developed information about the systematics of vibrational relaxation of diatomic ions with neutrals. It is clear that the newly developing field of molecular ion vibrational relaxation studies will provide useful insight into reaction dynamics, just as neutral vibrational relaxation studies have done for several decades.

#### APPENDIX

The modified monitor ion technique that is used to measure the quenching rate constants for the lower vibrational levels of O<sub>2</sub><sup>+</sup> when the upper states react with the quenching gas is demonstrated here for the simplified case of a three-state model.

[A<sup>+</sup>(0)]<sub>0</sub>, [A<sup>+</sup>(1)]<sub>0</sub>, and [A<sup>+</sup>(2)]<sub>0</sub> are the initial concentrations at the upstream end of the FDT of the ground state ions, the excited, unreactive ions, and the excited, reactive

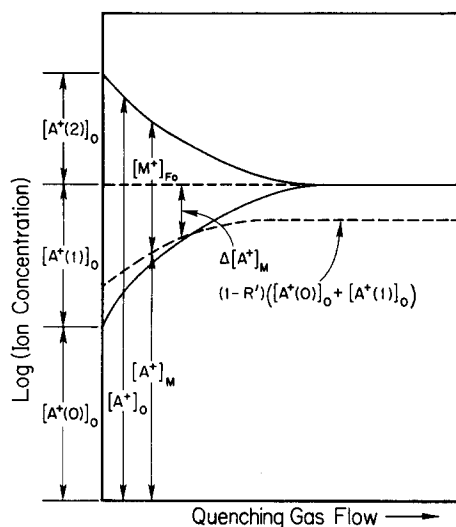


FIG. 11. Plot of ion concentrations as a function of quenching/reactant gas for the three-state system analyzed in Appendix A. [A<sup>+</sup>(*n*)]<sub>0</sub>, *n* = 0, 1, 2, are the initial concentrations for the three states of the primary ion A<sup>+</sup>. [A<sup>+</sup>]<sub>M</sub> and [A<sup>+</sup>]<sub>0</sub> are the concentrations of all A<sup>+</sup> ions at the FDT detector with and without monitor gas M added to the system. [M<sup>+</sup>]<sub>F0</sub> is the monitor ion concentration at the detector. Δ[A<sup>+</sup>]<sub>M</sub> is a difference concentration that is used to give the quenching rate of A<sup>+</sup>(1) ions when *R* is close to unity (see the Appendix).

ions, respectively. (Refer to Fig. 11.) With *Q* as the quenching/reactant gas, we have



[A<sup>+</sup>]<sub>0</sub> is the initial primary ion concentration that includes all states of the ion

$$[A^+]_0 = [A^+(0)]_0 + [A^+(1)]_0 + [A^+(2)]_0. \quad (\text{A4})$$

The concentration of A<sup>+</sup> ions in the flow tube is a function of the flow of quenching/reactant gas *Q* and the rate constants of Eqs. (A2) and (A3). We have then

$$[A^+] = [A^+(0)]_0 + [A^+(1)]_0 + [A^+(2)]_0 \exp(-\alpha\tau), \quad (\text{A5})$$

$$[A^+(0)] = [A^+(0)]_0 + [A^+(1)]_0(1 - \exp(-\beta\tau)), \quad (\text{A6})$$

where  $\alpha = k_r[Q]$ ,  $\beta = k_q[Q]$ , and  $\tau$  is the residence time of the ions in the drift-reaction region.

The monitor ion signal M<sup>+</sup> is produced from A<sup>+</sup> ions reacting with the monitor gas M. Both the excited state and ground state ions will, in general, react to produce M<sup>+</sup> ions. The fractions of excited state and ground state ions that react to produce M<sup>+</sup> are a function of the respective reaction rate constants with M and the flow of M. These fractions are designated *R* and *R'*, respectively, at a monitor flow *F*<sub>0</sub> [see Eqs. (A5) and (A6) in Ref. 5]. The concentrations of M<sup>+</sup> ions at the FDT detector is given by

$$[M^+]_{F_0} = R([A^+] - [A^+(0)]) + R'[A^+(0)], \quad (\text{A7})$$

where the A<sup>+</sup> concentrations are evaluated at the monitor gas inlet. Substituting Eqs. (A5) and (A6) in Eq. (A7), we obtain

$$[M^+]_{F_0} = [A^+(1)]_0(R - R')\exp(-\beta\tau) + R' + [A^+(2)]_0R\exp(-\alpha\tau) + R'[A^+(0)]_0. \quad (A8)$$

The addition of monitor gas to the FDT results in a reduction of  $A^+$  ions in the system. The concentration of  $A^+$  ions at the detector with monitor gas present is given by

$$[A^+]_M = [A^+] - [M^+]_0. \quad (A9)$$

Using Eqs. (A5) and (A7), we have

$$[A^+]_M = [A^+(0)]_0(1 - R) + [A^+(1)]_0 \times (1 - R' - (R - R')\exp(-\beta\tau)) + [A^+(2)]_0(1 - R)\exp(-\alpha\tau). \quad (A10)$$

When the flow of  $Q$  is large, the exponential terms vanish and Eq. (A10) reduces to a constant term that depends only on the monitor flow  $F_0$  through  $R$  and  $R'$ :

$$[A^+]_M = [A^+(0)]_0(1 - R) + [A^+(1)]_0(1 - R'), \quad (A11)$$

$[Q]$  large.

The difference between Eqs. (A11) and (A10), therefore, is a term that depends on  $Q$  and is defined as  $\Delta[A^+]_M$ . We then have

$$\Delta[A^+]_M = [A^+(1)]_0(R - R')\exp(-\beta\tau) - [A^+(2)]_0(1 - R)\exp(-\alpha\tau). \quad (A12)$$

In summary,  $\Delta[A^+]_M$  is the magnitude of the change in the  $A^+$  ion signal in the FDT detection system as a function of  $Q$  for fixed values of  $R$  and  $R'$  set by the monitor gas  $M$  at flow  $F_0$ .

Finally, if the monitor gas flow is sufficiently large,  $R$  can be made to be approximately unity (see Appendix A, Ref. 5), causing the second term of Eq. (A12) to vanish. For this condition, the change in the  $A^+$  ion signal is a pure exponential that depends only on the quenching rate constant  $k_q$  of  $A^+(1)$  ions, the desired result.

<sup>1</sup>I. Dotan, F. C. Fehsenfeld, and D. L. Albritton, *J. Chem. Phys.* **68**, 5665 (1978).

<sup>2</sup>D. L. Albritton, in *Kinetics of Ion-Molecule Reactions*, edited by P. Ausloos (Plenum, New York, 1979), p. 119.

<sup>3</sup>E. Alge, H. Villinger, and W. Lindinger, *Plasma Chem. Plasma Proc.* **1**, 65 (1981).

<sup>4</sup>M. Durup-Ferguson, H. Böhlinger, D. W. Fahey, and E. E. Ferguson, *J. Chem. Phys.* **79**, 265 (1983).

<sup>5</sup>H. Böhlinger, M. Durup-Ferguson, D. W. Fahey, F. C. Fehsenfeld, and E. E. Ferguson, *J. Chem. Phys.* **79**, 4201 (1983).

<sup>6</sup>H. Böhlinger, M. Durup-Ferguson, E. E. Ferguson, and D. W. Fahey, *Planet. Space Sci.* **31**, 483 (1983).

<sup>7</sup>W. Dobler, W. Federer, F. Howorka, W. Lindinger, M. Durup-Ferguson, and E. E. Ferguson, *J. Chem. Phys.* **79**, 1543 (1983).

<sup>8</sup>L. A. Viehland, S. L. Lin, and E. A. Mason, *Chem. Phys.* **54**, 341 (1981).

<sup>9</sup>M. McFarland, D. L. Albritton, F. C. Fehsenfeld, E. E. Ferguson, and A. L. Schmeltkopf, *J. Chem. Phys.* **59**, 6610, 6620, and 6629 (1973).

<sup>10</sup>D. W. Fahey, I. Dotan, F. C. Fehsenfeld, D. L. Albritton, and L. A. Viehland, *J. Chem. Phys.* **76**, 3320 (1981).

<sup>11</sup>G. Dupeyrat, B. R. Rowe, D. W. Fahey, and D. L. Albritton, *Int. J. Mass Spectrom. Ion Phys.* **44**, 1 (1982).

<sup>12</sup>W. Lindinger, D. L. Albritton, M. McFarland, F. C. Fehsenfeld, A. L. Schmeltkopf, and E. E. Ferguson, *J. Chem. Phys.* **62**, 4101 (1975).

<sup>13</sup>J. Glosik, A. B. Rakshit, N. D. Twiddy, N. G. Adams, and D. Smith, *J. Phys. B* **11**, 3365 (1978).

<sup>14</sup>P. H. Krupenic, *J. Phys. Chem. Ref. Data* **1**, 423 (1972).

<sup>15</sup>H. M. Rosenstock, K. Draxl, B. W. Steiner, and J. T. Herron, *J. Phys. Chem. Ref. Data Suppl.* **6**, 1 (1977).

<sup>16</sup>D. R. Stull and H. Prophet, *JANAF Thermochemical Tables*, 2nd ed., NSRDS Natl. Bur. Stand. No. 37 (U.S. GPO, Washington, D.C., 1971).

<sup>17</sup>F. M. Benoit, A. G. Harrison, and F. P. Lossing, *Organic Mass Spectrom.* **12**, 78 (1977).

<sup>18</sup>L. G. S. Shum and S. W. Benson, *J. Phys. Chem.* **87**, 3479 (1983).

<sup>19</sup>D. Smith, and N. G. Adams, *Int. J. Mass Spectrom. Ion Phys.* **23**, 123 (1977).

<sup>20</sup>H. Villinger, R. Richter, and W. Lindinger, *Int. J. Mass Spectrom. Ion Phys.* **51**, 25 (1983).

<sup>21</sup>H. Villinger, A. Saxer, R. Richter, and W. Lindinger, *Chem. Phys. Lett.* **96**, 513 (1983).

<sup>22</sup>L. A. Viehland and D. W. Fahey, *J. Chem. Phys.* **78**, 435 (1983).

<sup>23</sup>D. L. Albritton, I. Dotan, W. Lindinger, M. McFarland, J. Tellinghuisen, and F. C. Fehsenfeld, *J. Chem. Phys.* **65**, 410 (1977).

<sup>24</sup>E. E. Ferguson, in *Vibrational Excitation and Deexcitation and Charge-Transfer of Molecular Ions in Drift Tubes in Swarms of Ions and Electrons in Gases*, edited by W. Lindinger, T. D. Märk, and F. Howorka (Springer, Berlin, 1984).

<sup>25</sup>W. Dobler, W. Federer, W. Lindinger, M. Durup-Ferguson, and E. E. Ferguson, *J. Chem. Phys.* **79**, 1543 (1983).

<sup>26</sup>D. Smith, N. G. Adams, and T. M. Miller, *J. Chem. Phys.* **65**, 308 (1978).

<sup>27</sup>D. W. Fahey, F. C. Fehsenfeld, E. E. Ferguson, and L. A. Viehland, *J. Chem. Phys.* **75**, 669 (1981).

<sup>28</sup>B. R. Rowe, G. Dupeyrat, J. B. Marquette, D. Smith, N. Adams, and E. E. Ferguson, *J. Chem. Phys.* **80**, 241 (1984).

<sup>29</sup>I. Dotan, J. A. Davidson, F. C. Fehsenfeld, and D. L. Albritton, *J. Geophys. Res.* **83**, 4036 (1978).

<sup>30</sup>V. Nestler and P. Warneck, *Chem. Phys. Lett.* **45**, 96 (1977).

<sup>31</sup>K. Tanaka, T. Kato, and I. Koyano, *At. Collision Res. Jpn.* **9**, 73 (1983).